Postprint of: Mul M., Jasiński M., Lamęcki A., Gómez-García R., Mrozowski M., Inline Microwave Filters With N+1 Transmission Zeros Generated by Frequency-Variant Couplings: Coupling-Matrix-Based Synthesis and Design, IEEE TRANSACTIONS ON CIRCUITS AND SYSTEMS II-EXPRESS BRIEFS Vol. 69, iss. 3 (2022), pp. 824-828, DOI: 10.1109/TCSII.2021.3125460

Inline Microwave Filters With $N+1$ Transmission Zeros Generated by Frequency-Variant Couplings: Coupling-Matrix-Based Synthesis and Design

Martyna Mul, Maciej Jasinski, *Student Member, IEEE*, Adam Lamecki, *Senior Member, IEEE*, Roberto Gómez-García, *Senior Member, IEEE*, and Michal Mrozowski, *Fellow, IEEE*

***Abstract*—A general coupling-matrix-based synthesis methodology for inline Nth-order microwave bandpass filters (BPFs) with frequency-variant reactive-type couplings that generate $N+1$ transmission zeros (TZs) is presented in this brief. The proposed approach exploits the formulation of the synthesis problem as three inverse nonlinear eigenvalue problems (INEVPs) so that the coupling matrix is built from their sets of eigenvalues. For this purpose, an optimization nonlinear least-squares procedure is employed. The theoretical foundations of the engineered INEVP coupling-matrix-based synthesis framework are described. In addition, its effectiveness is verified through various synthesis examples of a third-order BPF with four TZs based on different circuit models. Moreover, as experimental validation, a 2.4-GHz microstrip prototype of the distributed-element BPF synthesis example is built and measured.**

***Index Terms*—Bandpass filter (BPF), coupling matrix, filter synthesis, microstrip filter, microwave filter, nonlinear eigenvalue problem (NEVP), RF filter, transmission zero (TZ)s.**

I. Introduction

HIGHLY-selective coupled-resonator-based microwave bandpass filters (BPFs) with generalized Chebyshev-type filtering response are required for RF front-ends in modern wireless-communication systems. Transmission zeros (TZs) are created in these BPFs to attain sharp-rejection capabilities by introducing couplings among non-adjacent resonators, as demonstrated by a plurality of static and frequency-tunable prior-art BPF designs [1]–[4]. The number of generated TZs and their locations depend on the coupling scheme, as well as on the strength and character of the couplings. Thus, a BPF network exhibiting N cross-couplings either of the inductive- or capacitive-type allows for $N-1$ TZs to be produced. Two additional TZs can be introduced in fully-canonical BPFs by adding resonant coupling between the source and the load [5], [6].

Inline BPF configurations with N resonators and $N+1$ TZs generated by frequency-variant—i.e., mixed—couplings have also been discussed in the technical literature and even confirmed by numerical simulations and experiments [7]–[10]. When compared to their cross-coupling counterparts that require several coupling paths among resonators, less complex and sensitive coupling-routing diagrams are attained as main benefits. However, despite their relevance and to the best of the authors' knowledge, no generalized design procedures based on coupling-resonator models have been proposed to date.

In this brief, a coupling-matrix-based synthesis approach for inline Nth-order BPFs with frequency-variant couplings and $N+1$ TZs is presented. The engineered optimization-based technique relies of the definition of the synthesis problem as a set of inverse nonlinear eigenvalue problems (INEVPs), from which the intended coupling matrix can be derived by using an iterative fast-convergence nonlinear least-squares solver. In addition to the INEVP framework used in the synthesis procedure, the novelty of this work is as follows: i) filtering functions with equiripple-type characteristics and prescribed level of minimum in-band insertion loss, N reflection zeros, and $N+1$ TZs are derived to provide the reference zeros and poles for the synthesis, ii) reactive inverters can have an arbitrary frequency-variation profile, iii) synthesis accounts for the dispersive TZ-generating input/output couplings, iv) ability to handle different models within a single coupling-matrix representation, and v) accounting for the strong resonator detuning effect due to their loading by inverters. These features are unique and their validity is verified with the synthesis of four BPF examples and with the fabrication and testing of a third-order inline BPF microstrip prototype with 4 TZs.

II. Theoretical Foundations

The scattering parameters of a filter network in the lowpass prototype domain Ω can be mathematically expressed as rational functions as follows:

$$S_{11}(\Omega)=\frac{F(\Omega)}{E(\Omega)}=1+\frac{F(\Omega)-E(\Omega)}{E(\Omega)},\quad S_{21}(\Omega)=\frac{P(\Omega)}{E(\Omega)} \tag{1}$$

where $F(\Omega), P(\Omega)$, and $E(\Omega)$ are polynomials and Ω is the normalized frequency. The roots of $P(\Omega)$ are TZs, whereas the roots of $F(\Omega)$ represent frequencies at which no power is reflected, or reflection zeros (RZs). At the same time, the power transmission properties of a filter can be expressed as

$$|S_{21}(\Omega)|^2=\frac{1}{1+\varepsilon^2 C^2(\Omega)} \tag{2}$$

where ε is a normalization constant that is related to the assumed maximum in-band power-insertion-loss level—or, equivalently, minimum in-band power-matching level [11]—and $C(\Omega)$ is a filtering function that adopts the following form for a filter with $N+1$ TZs:

$$C(\Omega)=\frac{\prod_{i=1}^{N}(\Omega-\Omega_{fi})}{\prod_{i=1}^{N+1}(\Omega-\Omega_{pi})}=\frac{F(\Omega)}{P(\Omega)}. \tag{3}$$

M. Mul, M. Jasinski, A. Lamecki, and M. Mrozowski are with the Faculty of Electronics, Telecommunications, and Informatics, Gdańsk University of Technology, 80-233 Gdansk, Poland (e-mail: martyna.mul@pg.edu.pl; maciej.jasinski@pg.edu.pl; adam.lamecki@ieee.org; m.mrozowski@ieee.org).

R. Gómez-García is with the Department of Signal Theory and Communications, Polytechnic School, University of Alcalá, 28871 Alcalá de Henares, Spain (e-mail: roberto.gomez.garcia@ieee.org).

This work was supported by the Polish National Science Centre under contract UMO-2019/33/B/ST7/00889.

© 2021 IEEE. Personal use of this material is permitted. Permission from IEEE must be obtained for all other uses, in any current or future media, including reprinting/republishing this material for advertising or promotional purposes, creating new collective works, for resale or redistribution to servers or lists, or reuse of any copyrighted component of this work in other works.

This article has been accepted for publication in a future issue of this journal, but has not been fully edited. Content may change prior to final publication. Citation information: DOI 10.1109/TCSII.2021.3125460, IEEE Transactions on Circuits and Systems II: Express Briefs

Polynomial $P(\Omega)$ is of the order $N+1$ and its roots Ω_{pi} are known and given by the $N+1$ TZs. On the other hand, polynomial $F(\Omega)$ is unknown and its roots Ω_{fi} have to be determined so as to ensure that the levels associated to all the in-band power-reflection maxima are identical. To synthesize the filtering function of a generalized Chebyshev filter with $N+1$ TZs, the optimization-based procedure developed in [6] for filters with resonant-type source-load coupling is used here. In this procedure the following cost function is minimized:

$$C_E = \sum_{n=1}^{N} |C(\Omega_{c_n}) - C(\Omega_{c_{n+1}})|^2 \tag{4}$$

where $\Omega_{cN} = -1$, $\Omega_{cN+1} = 1$, and Ω_{c_n} $(n = 1, 2, \ldots, N-1)$ are the locations of the in-band ripple maxima that are found by obtaining the roots of the derivative of $C(\Omega)$ as follows:

$$\frac{dC(\Omega)}{d\Omega} = F(\Omega)'P(\Omega) - P(\Omega)'F(\Omega) = 0. \tag{5}$$

Once polynomial $F(\Omega)$ is determined, then the third polynomial $E(\Omega)$ is obtained from the Feldkeller's equation [12].

To design a BPF with power transmission and reflection properties given by a predefined filtering function, a proper filtering network has to be synthesised. To this end, the recently-developed synthesis technique reported in [13] will be used, which achieves this goal by solving a suitably-defined INEVP. Using such INEVP framework for the synthesis allows for arbitrary-frequency-variation profiles for the couplings to be considered as long as they are reactive two-port networks. For a filtering network consisting of N resonators, the Kirchhoff's law in matrix formulation is given by the following expression:

$$[\mathbf{R} + j\mathbf{X}(\omega)]\,[i_S, i_1, i_2 \cdots, i_N, i_L]^T = [V_S, 0 \cdots, 0]^T \tag{6}$$

where ω is the angular frequency in the bandpass domain, $\mathbf{X}(\omega)$ is the $(N+2)\times(N+2)$ frequency-dependent coupling matrix, $\mathbf{R}$ is the $(N+2)\times(N+2)$ matrix that is zero except for the first and last elements on the main diagonal—that are set by the internal resistances of the source and the load, R_S and R_L, respectively—, V_S is the source voltage, and $i_S, i_1, i_2, \ldots, i_N, i_L$ are the loop currents. The scattering parameters for this network can be derived from (6) as follows:

$$S_{11}(\omega) = 1 + 2jR_S \frac{\det(\mathbf{X}'(\omega) - j\mathbf{R}')}{\det(\mathbf{X}(\omega) - j\mathbf{R})} \tag{7}$$

$$S_{21}(\omega) = -2j\sqrt{R_S R_L} \frac{\det(\mathbf{X}''(\omega) - j\mathbf{R}'')}{\det(\mathbf{X}(\omega) - j\mathbf{R})} \tag{8}$$

where the prime symbol denotes a matrix with the first row and first column removed, while the double prime refers to a matrix with the first row and last column removed.

By comparing the above expressions with (1), it becomes evident that the zeroes of the determinants in the numerators and denominators coincide with the roots of the polynomials occurring in the rational representations (1). At the same time, the zeros of the determinants are defined by the eigenvalues of the following nonlinear eigenvalue problems (NEVPs):

$$(\mathbf{X}'(\omega) - j\mathbf{R}')\mathbf{x} = 0 \tag{9}$$

$$(\mathbf{X}''(\omega) - j\mathbf{R}'')\mathbf{x} = 0 \tag{10}$$

$$(\mathbf{X}(\omega) - j\mathbf{R})\mathbf{x} = 0. \tag{11}$$

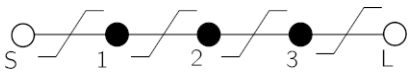

Fig. 1. Coupling-routing diagram of the inline third-order BPF with four TZs to be synthesized (black circles: resonators; white circles: source and load; continuous lines with step symbol: frequency-variant couplings).

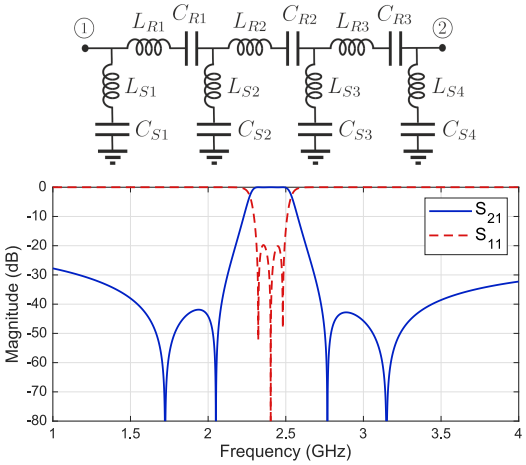

Fig. 2. Synthesized lumped-element BPF realization: circuit network, power transmission ($|S_{21}|$) and reflection ($|S_{11}|$) responses ($L_{S1} = 2.2266$ nH, $C_{S1} = 3.8316$ pF, $L_{R1} = 1.0958$ nH, $C_{R1} = 1.9924$ pF, $L_{S2} = 0.982$ nH, $C_{S2} = 6.1382$ pF, $L_{R2} = 1.2431$ nH, $C_{R2} = 3.5204$ pF, $L_{S3} = 0.7916$ nH, $C_{S3} = 4.1763$ pF, $L_{R3} = 1.7447$ nH, $C_{R3} = 6.7348$ pF, $L_{S4} = 1.4717$ nH, and $C_{S4} = 1.7356$ pF).

The synthesis technique developed in [13] uses the roots of polynomials $F(\omega) - E(\omega), P(\omega)$, and $E(\omega)$ and solves the above NEVPs for an unknown matrix $\mathbf{X}(\omega)$. That is, it finds the elements of matrix $\mathbf{X}(\omega)$ that, for a given network topology and reactances providing frequency-variant couplings and with three sets of eigenvalues known from the roots of polynomials $F(\omega) - E(\omega), P(\omega)$, and $E(\omega)$, fulfill the three NEVPs (9)–(11). To this end, a nonlinear optimization process is used.

III. Synthesis Examples

An inline filter topology is considered in the synthesis examples of this work, whose coupling matrix is tri-diagonal and symmetric with network nodes—i.e., resonators—on the main diagonal and couplings represented by the sub-diagonal elements as formulated in (12).

$$\mathbf{X}(\omega) = \begin{bmatrix} x_{SS} & x_{S1} & & & & & 0 \\ x_{S1} & x_{11} & x_{12} & & & & \\ & \ddots & \ddots & \ddots & & & \\ & & & x_{(N-1)N} & x_{NN} & x_{NL} & \\ 0 & & & & x_{NL} & x_{LL} & \end{bmatrix}. \tag{12}$$

To clearly separate the reactances at the network nodes or resonators from the couplings, it is convenient to split the previous matrix (12) as follows:

$$j\mathbf{X}(\omega) = j\mathbf{X}^r + j\mathbf{X}^c \tag{13}$$

where $\mathbf{X}^r$ is the diagonal matrix of reactances at each node and $\mathbf{X}^c$ is the tri-diagonal matrix related to couplings.

MOST WIEDZY Downloaded from mostwiedzy.pl

9-7747 (c) 2021 IEEE. Personal use is permitted, but republication/redistribution requires IEEE permission. See http://www.ieee.org/publications_standards/publications/rights/index.html for more information.
Authorized licensed use limited to: Politechnika Gdanska. Downloaded on November 29,2021 at 16:56:35 UTC from IEEE Xplore. Restrictions apply.

This article has been accepted for publication in a future issue of this journal, but has not been fully edited. Content may change prior to final publication. Citation information: DOI 10.1109/TCSII.2021.3125460, IEEE Transactions on Circuits and Systems II: Express Briefs

The design of an inline BPF with $N+1$ TZs and N in-band RZs will be illustrated for the particular case involving $N=3$ resonators. The coupling-routing diagram of this filter is shown in Fig. 1. As can be seen, there are three resonators with a frequency-variant inverter between each pair of them. Additionally, there are two frequency-variant inverters that are located between the source and resonator 1 and resonator 4 and the load. Each inverter exhibits nonlinear frequency-dependent variation and its role is to couple the two involved nodes—i.e., resonators and/or source and load—while producing a TZ at the same time to attain a total of $N+1=4$ out-of-band TZs.

The BPF is specified to be centered at 2.4 GHz with a ripple-referred fractional bandwidth of 7.5%—i.e., absolute bandwidth of 180 MHz—, and a minimum in-band return-loss level of 20 dBs. The four TZs are intended to be located at 1.72 GHz, 2.05 GHz, 2.77 GHz, and 3.15 GHz. In particular, three different models or realizations in the synthesis of this BPF will be shown, as follows: (i) lumped-element filter, (ii) mixed-element/semi-distributed-element filter with lumped-element series-type resonators and couplings based on shunt quarter-wavelength open-ended stubs, and (iii) fully-distributed filter with half-wavelength transmission-line resonators and shunt quarter-wavelength open-ended stubs for the couplings (two variants). In all cases, the coupling networks—i.e., shunt lumped-element series-type resonators or shunt quarter-wavelength open-ended stubs—create TZs. The source and load impedances are $R_S=R_L=Z_0=50\ \Omega$. For the coupling-routing diagram shown in Fig. 1 and the couplings being reactive two-port networks with open-circuit impedance elements $z_{11}^{(k)}=z_{22}^{(k)}=z_{21}^{(k)}=z_{12}^{(k)}=Z_k$ $(k=1,2,3,4)$, the elements of matrices $j\mathbf{X}^r$ and $j\mathbf{X}^c$ are given by

$$x_{SS}^r=x_{LL}^r=0 \text{ and } jx_{ii}^r=Z_{Ri} \tag{14}$$

$$jx_{12}^c=jx_{21}^c=-Z_2, \quad jx_{23}^c=jx_{32}^c=-Z_3 \tag{15}$$

$$jx_{S1}^c=jx_{1S}^c=-Z_1, \quad jx_{3L}^c=jx_{L3}^c=-Z_4 \tag{16}$$

and

$$jx_{SS}^c=Z_1, \quad jx_{LL}^c=Z_4, \quad jx_{ii}^c=Z_i+Z_{(i+1)}. \tag{17}$$

Note that in the above equations $i=1,2,3$, while the expressions for Z_{Ri} and Z_k depend on the selected implementation.

A. Reference Zeros and Poles

The characteristic polynomials were calculated using the procedure developed in [6] as previously indicated. The reference zeros and poles to be used in the synthesis examples (defined in the bandpass domain and with values given in GHz) are listed in Table I. As can be seen, polynomials $P(\omega)$ and $E(\omega)$ are of the fourth order, but there are three in-band RZs, four TZs, three in-band poles, and one extra pole appearing in the proximity of the zero frequency.

B. Example 1: Lumped-Element Model

As the first synthesis example, a lumped-element BPF model is considered. In this case, the involved reactive impedance elements are given by the following expressions:

$$Z_{Ri}=j\omega L_{Ri}-\frac{j}{\omega C_{Ri}} \quad Z_k=j\omega L_{Sk}-\frac{j}{\omega C_{Sk}} \tag{18}$$

TABLE I
REFERENCE ZEROS AND POLES (IN GHZ)

Zeros of F	Zeros of P	Zeros of E	Zeros of $F-E$
2.3232	1.7230	2.2812 + j0.0471	2.2843 +j0.0190
2.4801	2.0499	2.4015 + j0.1127	2.4023 + j0.0660
2.4016	2.7681	2.5222 + j0.0475	2.5203 + j0.0186
	3.1491	0.0004 + j0.0780	0.0001 + j0.0389

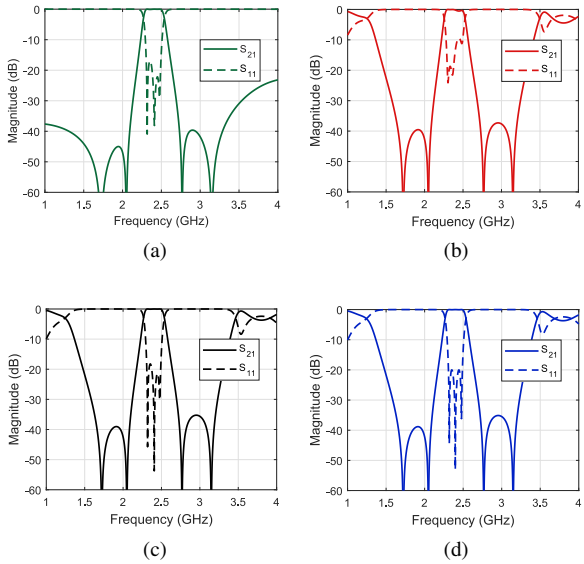

Fig. 3. Power transmission ($|S_{21}|$) and reflection ($|S_{11}|$) responses of the synthesised BPFs. (a) Mixed-element model. (b) Fully-distributed-element model (variant A). (c) Fully-distributed-element model (variant B) before final tuning. (d) Fully-distributed-element model (variant B) after final tuning.

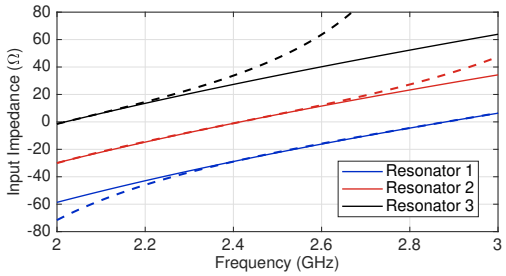

Fig. 4. Input-impedance frequency-variation profiles of the three resonators used in the synthesis examples in Sections II-C and II-D (solid lines: LC resonators; dashed lines: half-wavelength transmission-line resonators).

with $i=1,2,3$ and $k=1,2,3,4$. In this example, the frequency-variant couplings are realized as series-type LC resonators. When solving the associated INEVP, the values for the lumped capacitances and inductances were set as optimization variables. The results derived from the synthesis process in terms of lumped-element circuit network and associated power transmission and reflection responses are represented Fig. 2. As can be seen, the prefixed specifications are fully satisfied.

C. Example 2: Mixed-Element Model

In this second synthesis example, the reactances of the network nodes are not specified but they are assumed to be resonating elements at the angular frequency ω_i that have a

MOST WIEDZY Downloaded from mostwiedzy.pl

9-7747 (c) 2021 IEEE. Personal use is permitted, but republication/redistribution requires IEEE permission. See http://www.ieee.org/publications_standards/publications/rights/index.html for more information.
Authorized licensed use limited to: Politechnika Gdanska. Downloaded on November 29,2021 at 16:56:35 UTC from IEEE Xplore. Restrictions apply.

This article has been accepted for publication in a future issue of this journal, but has not been fully edited. Content may change prior to final publication. Citation information: DOI 10.1109/TCSII.2021.3125460, IEEE Transactions on Circuits and Systems II: Express Briefs

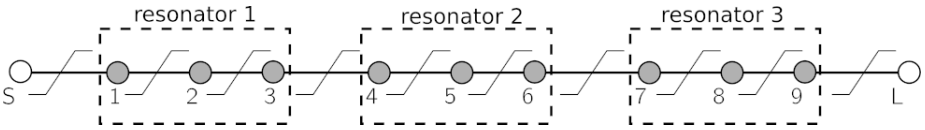

Fig. 5. Coupling-routing diagram of the alternative representation for the inline third-order BPF with four TZs to be synthesized using non-resonating nodes (grey circles: non-resonating nodes; white circles: source and load; continuous lines with step symbol: frequency-variant couplings).

TABLE II
PARAMETERS OF THE INVERTERS: LINE IMPEDANCES (IN Ω) AND ELECTRICAL LENGTHS OF THE STUBS AT THE CENTER FREQUENCY f_c (IN DEGREES)

Model	Z_{S1}	Z_{S2}	Z_{S3}	Z_{S4}	$\theta_{S1}(f_c)$	$\theta_{S2}(f_c)$	$\theta_{S3}(f_c)$	$\theta_{S4}(f_c)$
Mixed-element	40.7116	45.0758	55.0289	69.4065	125.3582	105.4047	78.0422	68.5980
Distributed-element (variant B)	42.1264	42.783	59.1312	83.0321	125.3582	105.4047	78.0422	68.5980
Distributed-element (variant B) tuned	42.5797	42.783	59.6398	83.9473	125.3582	105.4047	78.0422	68.5980

TABLE III
RESONANT FREQUENCIES OF THE RESONATORS (IN GHZ)

Model	f_{R1}	f_{R2}	f_{R3}
Mixed-element	2.8815	2.4160	2.0186
Distributed-element (variant B)	2.9376	2.3953	2.0245
Distributed-element (variant B) tuned	2.93115	2.39259	2.02054

reactance-slope parameter at resonance given by χ. Unlike in the previous design example where lumped elements were utilized to implement the coupling networks, the frequency-variant couplings are now realized as open-ended quarter-wavelength stubs. Thus, the following formulas are obtained in this case for the associated reactive impedance elements:

$$Z_{Ri} = j\chi\left(\frac{\omega}{\omega_i} - \frac{\omega_i}{\omega}\right) \quad Z_k = -jZ_{Sk}\cot\left(\frac{\omega\theta_{Sk}(\omega_c)}{\omega_c}\right) \tag{19}$$

with $i = 1, 2, 3$, $k = 1, 2, 3, 4$, and $\chi = 50\pi/2$.

The optimization variables for solving the INEVP are now the line impedances and electrical lengths of the stubs—i.e., Z_{S1}, Z_{S2}, Z_{S3}, Z_{S4}, and θ_{S1}, θ_{S2}, θ_{S3}, θ_{S4}—and the resonant frequencies—i.e., f_{R1}, f_{R2}, and f_{R3}. The results derived from the optimization, i.e., the optimum values of all variables, are given in the first row of Tables II and III. Note that resonators 1 and 3 are strongly detuned as a result of loading the resonators by the coupling elements—i.e., stubs. This effect is automatically taken into account in the synthesis procedure based on the INEVP framework by splitting (13). The power transmission and reflection responses of the synthesized BPF calculated from the final coupling matrix are depicted in Fig. 3(a). Note that some minor discrepancies are observed when compared to the results in Fig. 2, which are attributed to the different type of frequency dependence of LC and stub-based inverters.

D. Example 3: Fully-Distributed-Element Model (Variant A)

The third synthesis example consists of a fully-distributed BPF in a transmission-line realization, which is more appropriate for the microwave range. The LC resonators of the previous mixed-element model, which are characterized by their resonant frequencies ω_i and their identical reactance slopes at resonance $\chi = 50\pi/2$, are now replaced by half-wavelength transmission-line resonators with 50-Ω line impedance so that they exhibit the same reactance slope $\chi = 50\pi/2$ at the resonant frequency. Note that this is a standard step in the synthesis of microwave filters based on a coupling-matrix formalism [12].

The power transmission and reflection parameters of this transmission-line BPF realization with half-wavelength resonators are shown in Fig. 3(b). As can be seen, when compared to the curves plotted in Fig. 3(a), the in-band power-matching profile is significantly deteriorated—among some other deviations. This is due to the fact that the resonant frequencies are strongly detuned from the center frequency. Such detuning leads to discrepancies since the half-wavelength transmission-line resonator accurately represents its LC counterpart just at the resonant frequency and its vicinity. This is illustrated in Fig. 4, where the frequency-variation profiles of the input impedances for both types of resonators are compared.

E. Example 4: Fully-Distributed-Element Model (Variant B)

The previous design example has revealed an undesired in-band-response deterioration effect due to the different frequency-variation profiles of transmission-line resonators and their LC versions when they are strongly detuned. To circumvent this issue, a different distributed-element model is adopted here, in which each resonator is replaced by three non-resonating nodes coupled by two inverters (see Fig. 5) that are implemented as quarter-wavelength transmission-line sections. Non-resonating nodes can be readily accommodated in the proposed INEVP synthesis framework, since the only modification to be introduced is that the elements in matrix $j\mathbf{X}^r$ corresponding to these nodes must be set equal to zero [13]. Since each half-wavelength resonator is split in three non-resonating nodes and two inverters—i.e., quarter-wavelength sections—, matrix $j\mathbf{X}^r$ becomes zero and the size of the coupling matrix $j\mathbf{X}^c$ is 11×11.

The results derived from the INEVP synthesis procedure with this alternative representation are shown in the second row of Tables II and III. As can be seen in Fig. 3(c) where the resulting power transmission and reflection responses are plotted, the in-band behavior has been considerably improved. Furthermore, a very-minor final tuning was carried out to more-finely adjust these results as demonstrated in Fig. 3(d). The final values for the filter parameters associated to this very-slightly-tuned BPF example are provided in the last row of Tables II and III.

MOST WIEDZY Downloaded from mostwiedzy.pl

9-7747 (c) 2021 IEEE. Personal use is permitted, but republication/redistribution requires IEEE permission. See http://www.ieee.org/publications_standards/publications/rights/index.html for more information.
Authorized licensed use limited to: Politechnika Gdanska. Downloaded on November 29,2021 at 16:56:35 UTC from IEEE Xplore. Restrictions apply.

This article has been accepted for publication in a future issue of this journal, but has not been fully edited. Content may change prior to final publication. Citation information: DOI 10.1109/TCSII.2021.3125460, IEEE Transactions on Circuits and Systems II: Express Briefs

IV. Experimental Results

As practical demonstration of the fully-distributed-element BPF that was synthesized in Section III-E—tuned—, a proof-of-concept prototype has been developed in microstrip technology and tested. For its design, an Isola substrate with dielectric thickness $H = 0.762$ mm, relative dielectric permittivity $\varepsilon_r = 3.45$ (± 0.05), dielectric loss tangent $\tan(\delta_D) = 0.0035$, and metallization thickness $t = 17.5$ μm was utilized.

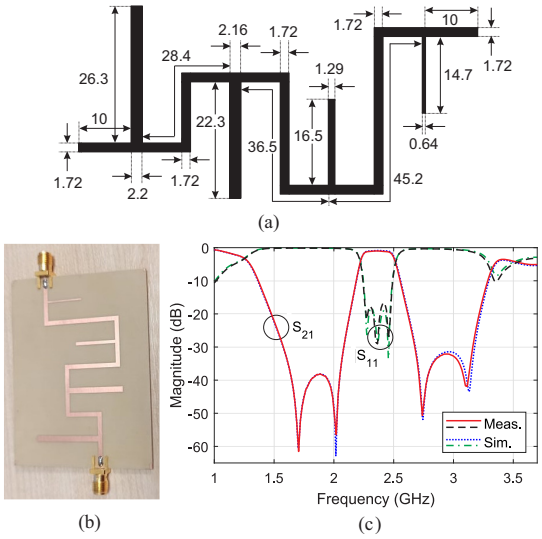

Fig. 6. Manufactured microstrip BPF prototype. (a) Layout (dimensions in mm). (b) Photograph. (c) Simulated and measured power-transmission ($|S_{21}|$) and reflection ($|S_{11}|$) responses.

The layout (with indication of dimensions) and a photograph of the manufactured microstrip BPF prototype, along with its simulated (with Ansys HFSS) and measured power transmission and reflection responses, are shown in Fig. 6. As can be seen, a fairly-close agreement between predicted and experimental results is obtained. The main measured performance metrics of this circuit are as follows: center frequency of 2.37 GHz, 3-dB bandwidth equal to 286 MHz—i.e., 12.1% in relative terms—, minimum in-band power-insertion-loss and power-matching levels of 1 dB and 16.5 dB, respectively, and TZs located at 1.71 GHz, 2 GHz, 2.74 GHz, and 3.11 GHz.

V. Conclusion

This brief has reported a generalized coupling-matrix-based synthesis approach for Nth-order microwave BPFs with $N + 1$ TZs on an inline topology with frequency-variant couplings. The proposed optimization-based synthesis methodology builds upon an INEVP formulation of the synthesis problem, which allows to obtain the targeted coupling matrix from three different sets of eigenvalues. The efficacy of the devised synthesis methodology and its universality have been proven through several BPF synthesis examples with different circuit models. Furthermore, a 2.4-GHz microstrip prototype of the synthesized transmission-line-based BPF has been built and tested for practical-validation purposes. Such optimization-based design approach is fully general to synthesize other classes of BPFs, including its extension to multi-band BPFs and multiplexers as further research work to be carried out.

References

[1] A. I. Abunjaileh and I. C. Hunter, "Direct synthesis of parallel-connected symmetrical two-port filters," *IEEE Trans. Circuits Syst. II, Exp. Briefs,* vol. 57, no. 12, pp. 971–974, Dec. 2010.

[2] A. Saghir, A. Quddious, S. Arain, P. Vryonides, and S. Nikolaou, "Single-/dual-BPF using coupled-line stepped impedance resonators (CLSIR)," *IEEE Trans. Circuits Syst. II, Exp. Briefs,* vol. 66, no. 9, pp. 1497–1501, Sep. 2019.

[3] S. Arain, P. Vryonides, A. Quddious, and S. Nikolaou, "Reconfigurable BPF with constant center frequency and wide tuning range of bandwidth," *IEEE Trans. Circuits Syst. II, Exp. Briefs,* vol. 67, no. 8, pp. 1374–1378, Aug. 2020.

[4] R. S. Sangam, S. Dash, and R. S. Kshetrimayum, "Ultra-broadband bandpass filter using linearly tapered coupled-microstrip line and open loop defected ground structure," *IEEE Trans. Circuits Syst. II, Exp. Briefs,* vol. 68, no. 1, pp. 181–185, Jan. 2021.

[5] R. Levy, "New cascaded trisections with resonant cross-couplings (ctr sections) applied to the design of optimal filters," in *IEEE MTT-S Int. Microw. Symp. Dig.,* vol. 2, 2004, pp. 447–450.

[6] L. Szydlowski, A. Lamecki, and M. Mrozowski, "A novel coupling matrix synthesis technique for generalized Chebyshev filters with resonant source–load connection," *IEEE Trans. Microw. Theory Techn.,* vol. 61, no. 10, pp. 3568–3577, Oct. 2013.

[7] J. J. Vague, D. Rubio, M. A. Fuentes, S. Cogollos, M. Baquero, V. E. Boria, and M. Guglielmi, "Inline combline filters of order N with up to $N + 1$ transmission zeros," *IEEE Trans. Microw. Theory Techn.,* vol. 69, no. 7, pp. 3287–3297, Jul. 2021.

[8] M. Y. Sandhu, Z. Ahmed, S. Hyder, and S. Afridi, "Inline integrated ceramic waveguide bandpass filter with $N + 1$ finite transmission zeros," *IETE J. Research,* pp. 1–7, 2020.

[9] D. Deslandes, "Bandpass filter with $N + 1$ transmission zeroes using frequency-variant couplings," in *Proc. 8th IEEE Int. New Circuits Syst. Conf. (NEWCAS),* Jun. 2010, pp. 217–220.

[10] A. Zakharov, S. Rozenko, L. Pinchuk, and S. Litvintsev, "Microstrip quazi-elliptic bandpass filter with two pairs of antiparallel mixed-coupled SIRs," *IEEE Microw. Wireless Compon. Lett.,* vol. 31, no. 5, pp. 433–436, May. 2021.

[11] R. J. Cameron, "General coupling matrix synthesis methods for Chebyshev filtering functions," *IEEE Trans. Microw. Theory Techn.,* vol. 47, no. 4, pp. 433–442, Apr. 1999.

[12] R. Cameron, C. Kudsia, and R. Mansour, *Microwave Filters for Communication Systems.* New York: Wiley, 2007.

[13] M. Mul, A. Lamecki, R. Gómez-García, and M. Mrozowski, "Inverse nonlinear eigenvalue problem framework for the synthesis of coupled resonator filters with non-resonant nodes and arbitrary frequency-variant reactive couplings," *IEEE Trans. Microw. Theory Techn.,* 2021, (Early access).

MOST WIEDZY Downloaded from mostwiedzy.pl

9-7747 (c) 2021 IEEE. Personal use is permitted, but republication/redistribution requires IEEE permission. See http://www.ieee.org/publications_standards/publications/rights/index.html for more information.
Authorized licensed use limited to: Politechnika Gdanska. Downloaded on November 29,2021 at 16:56:35 UTC from IEEE Xplore. Restrictions apply.